Lawrence Berkeley National Laboratory

Title
Design of a Reacceleration Experiment Using the Choppertron

Permalink
https://escholarship.org/uc/item/1x42p0nm

Author
Fiorentini, G.

Publication Date
1993

Lawrence Berkeley Laboratory
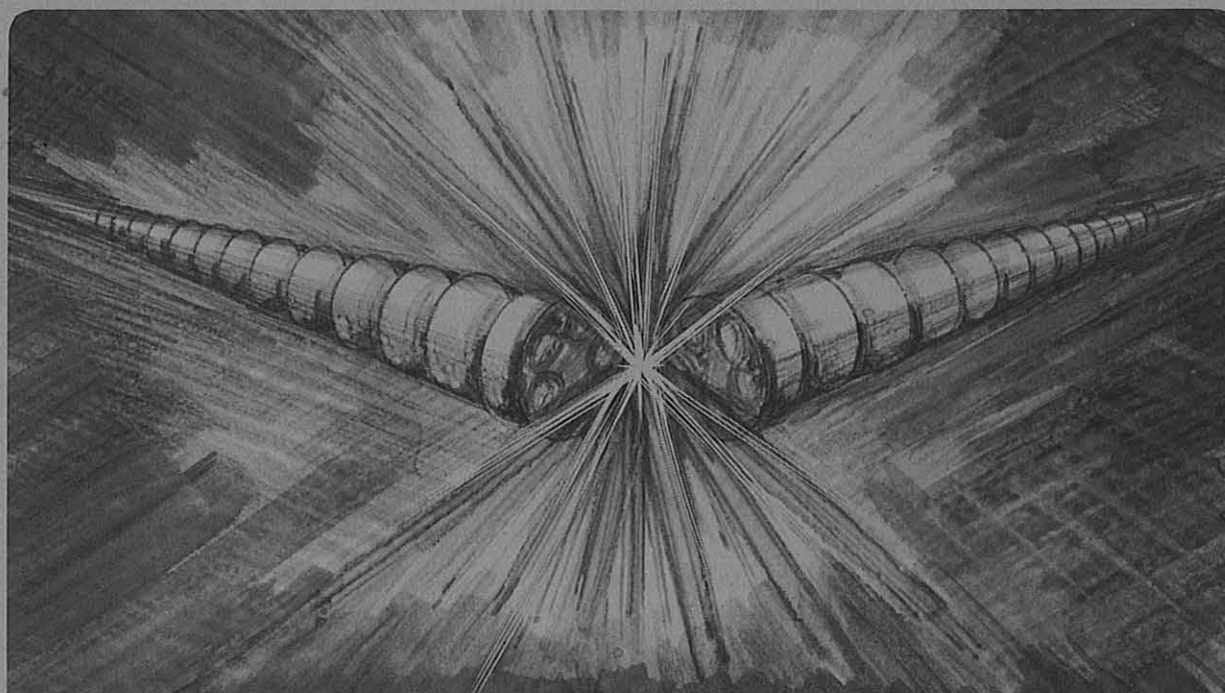## UNIVERSITY OF CALIFORNIA

Accelerator & Fusion Research Division

Presented at the SPIE's International Symposia on Laser Engineering, Los Angeles, CA, January 16–23, 1993, and to be published in the Proceedings

Design of a Reacceleration Experiment Using the Choppertron

G.M. Fiorentini, C. Wang, and T.L. Houck

January 1993

Design of a Reacceleration Experiment Using the Choppertron*

G.M. Fiorentini and C. Wang

Lawrence Berkeley Laboratory, University of California, Berkeley, California 94720

T.L. Houck

Lawrence Livermore National Laboratory, University of California, Livermore, California 94550

January 1993

MASTER

Design of a Reacceleration Experiment Using the Choppertron*

G. M. Fiorentini[†1], T. L. Houck[†2], and C. Wang[†3]

Lawrence Berkeley Laboratory
University of California, Berkeley, California 94720

ABSTRACT

The Microwave Source Facility at the Lawrence Livermore National Laboratory is commencing a series of experiments involving reacceleration of a modulated beam alternating with extraction of energy in the form of X-band microwaves. The Choppertron, a high-power microwave generator, is used to modulate a 5-MV, 1-kA induction accelerator beam. The modulated beam is then passed through a series of traveling-wave output structures separated by induction cells. In this paper we report on computer simulations used in the design of these experiments. Simulations include analysis of beam transport, modulation, power extraction and transverse instabilities.

1. INTRODUCTION

A collaboration between the Lawrence Livermore National Laboratory and the Lawrence Berkeley Laboratory has been studying microwave sources which could be suitable drivers for a future TeV linear e^+e^- collider. The Choppertron,[1] a high-power microwave generator which uses transverse modulation of the drive beam, has been successfully tested at the Microwave Source Facility.[2,3] Although the Choppertron has demonstrated high-power pulses, >150 MW per output at 11.424 GHz with stable phase and amplitude and >400 MW total peak power, the conversion efficiency of beam energy to microwaves is only about 30%. The efficiency could be significantly improved by reaccelerating the beam and extracting additional power. The application of this concept to a linear collider is referred to as the Relativistic Klystron Two-Beam Accelerator (RK-TBA).[4]

We are designing an experiment based on the Choppertron to study the reacceleration of a modulated beam as a verification of the feasibility of building a RK-TBA. Fig. 1 shows a layout of the proposed reacceleration experiment. The major experimental components, except for the induction accelerator that generates the drive beam, are shown in the layout. These components include the Choppertron beam modulator, traveling-wave microwave extraction structures, and induction cells for reacceleration. In addition to the induction cells, modifications to the original Choppertron experiment included: increasing the beam energy to compensate for longitudinal space charge effects over the longer output section; de-Q-ing circuits in the first two traveling-wave circuits to control growth of transverse instabilities; lengthening the modulator section to accommodate the higher beam energy; increasing the modulator drive power to adjust for larger than anticipated beam emittance. Our simulations indicate relatively consistent power extraction of 100 - 150 MW from each output and no beam breakup due to excitation of higher order modes in the traveling-wave structures.

2. MAJOR COMPONENTS OF THE REACCELERATION EXPERIMENT

The Choppertron was tested at the Microwave Source Facility at the Lawrence Livermore National Laboratory. The facility uses the Advanced Test Accelerator[5] (ATA) injector to supply a 1-kA, 2.5-MeV electron beam. For the reacceleration experiment it was desired to use as much of the original Choppertron

experiment as possible and modify existing equipment when needed. This had the effect of limiting the current to 1 kA, maximum design value for the modulator, and the beam emittance to that obtainable with the currently installed injector electrode package.
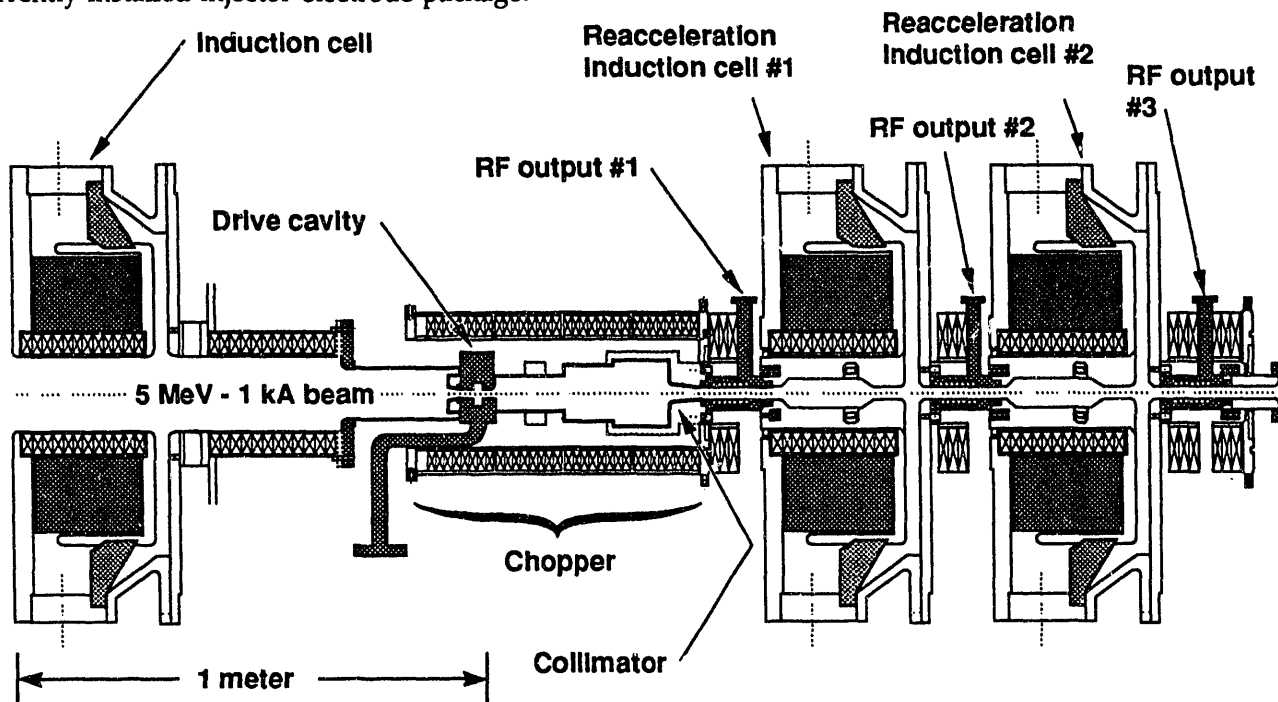

Figure 1. Schematic of proposed reacceleration experiment.

2.1 Drive Beam

Initial simulations using a one-dimensional klystron code showed a significant decrease in the available beam power for extraction due to debunching of the modulated beam by longitudinal space charge effects. Fig. 2 illustrates these effects on available microwave power (modulated current) as a function of beam energy for different modulated currents. In the simulation the extraction ports are spaced about every 0.5 m (a physical constraint imposed by the induction cell size to be used in the experiment) and the average beam energy was reduced by approximately 0.4 MeV with peak loss of 0.8 MeV in each extraction structure. Thus starting with a 2.5-MeV, 1-kA peak current beam, the energy was reduced to about 2 MeV almost immediately after the modulation section as the beam traversed the first traveling-wave structure. For the simulation (and the proposed experiment) there is no additional bunching of the beam after the modulation section so only about 50% of the power would be available for extraction at the second port as from the first due to space charge debunching with even lower power available at the third port. To avoid the power drop, the current could be reduce which would mean less total power extracted, the beam energy could be increased, and/or new traveling-wave structures could be constructed with effective impedances matched to the anticipated rf current.

We chose to design for increased energy. A 10-induction cell module, which increases the beam energy by 2.5 MeV, was placed after the injector. The total beam energy for the reacceleration experiment is 5.0 MeV .

Focusing and transport of the beam in the actual experiment is planned to be accomplished by a total of 34 solenoids prior to the modulator, five solenoids in the modulating section, and an additional six solenoids in the extraction section. Current and initial beam radius is determined by a 2-cm diameter, 1-m long pipe surrounded by four solenoids and located between the injector and the 10-induction cell module. This pipe acts as an emittance selector. Measurements indicate that at 1 kA the induction beam has a normalized emittance of about 104 π-cm-mr.[6] By varying the field of the solenoids, the amount of current transported through the pipe is adjusted from the 8 kA emitted from the cathode to the desired quantity.

A transport code based on the envelope equation[7,8] for the beam radius in a solenoidal magnetic field was used to simulate the transport of the beam and determine approximate current levels for the solenoids. An average field of 800 Gauss was found to keep the beam radius between 1 and 1.2 cm for 1 kA of current from the emittance selector through the ten-cell accelerating module. After the ten-cell module, the axial magnetic field was gradually increased to 1.2 kG in the simulation to decrease the beam radius to about 5.7 mm and match the beam into the modulator section. Transport of the beam through the microwave extraction section will be discussed in section 2.5.
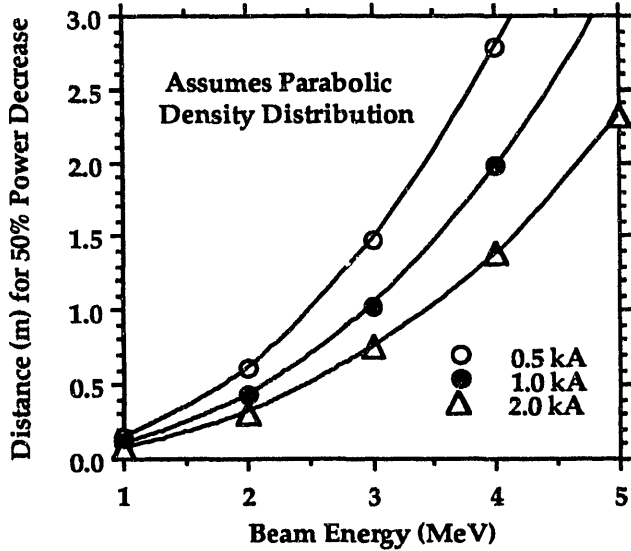

Figure 2. Loss of extractable rf power for a drifting beam due to longitudinal space charge effects.

Figure 3. Schematic of the original Choppertron.

2.2 Modulator

The Choppertron modulator has been analyzed elsewhere.[9] We will not attempt a detail design analysis of the modulating system as our intent was to use the existing modulator with minimum modification. A schematic of the original Choppertron is shown in Fig. 3. The modulator of the Choppertron is a 5.7-GHz chopping system designed to produce a train of short beam pulses with a period corresponding to 11.4 GHz from the initial uniform beam. The chopper design has reduced sensitivity to the induction beam-energy sweep. Emittance growth is reduced by matching the axial magnetic field in the drift section to the beam emittance and betatron resonance. The dc current is reduced by about half when the beam is fully modulated. Our major constraints were the deflection cavity (maximum deflection field) and solenoids (maximum axial magnetic field). When the Choppertron was initially constructed some provisions were made to allow for future operation at beam energies of 6 MeV. Specifically, the drift section was designed so that extensions could be readily inserted and additional solenoids were fabricated. By using existing parts it was possible to lengthen the drift distance to 54.7 cm. The greater length allows operation at slightly lower solenoidal fields and reduced drive power to the deflecting cavity assuming the beam radius can be maintained at the original design value of about 4 mm.

This assumption was based on a desired normalized beam edge emittance of 30 π-cm-mr. The Choppertron was designed and constructed to operate with this emittance. To appreciate the implications of this statement it is necessary to consider two pertinent equations. First is the envelope equation for the radius of a beam in a solenoidal magnetic field which can be expressed as:

$$R'' + \left(\frac{e\,B_z}{2\,\gamma\beta\,mc}\right)^2 R - \frac{\varepsilon_N^2}{\gamma^2\,\beta^2\,R^3} = \frac{2\,I}{17\,(\gamma\beta)^3\,R}, \text{ where} \tag{1}$$

ε_N is normalized emittance (m-rad), R is the beam radius (m), I is beam current (kA), B_z is the axial magnetic field (T), e/m denote the electron charge/mass (coulomb/kg), and prime denotes a derivative with respect to z, the longitudinal dimension. We take ε_N to be the edge emittance and R to be the maximum radius of the beam.
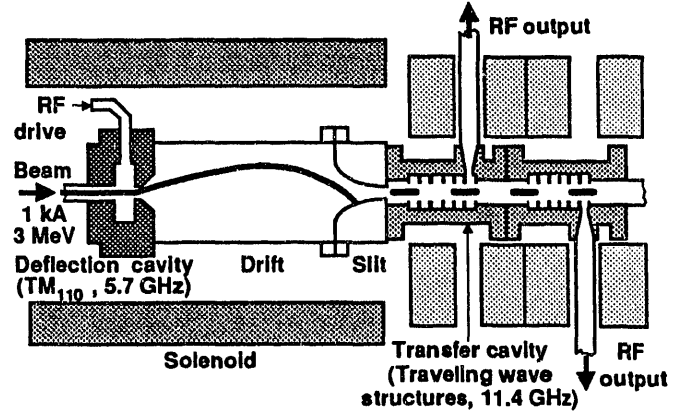
3

Although equation (1) is based on rms values of the parameters, our values should be proportional to the rms values with multiplicity constants depending on the cross sectional charge distribution. As the charge distribution is not well known, we have chosen our definition to be consistent with the method used to measure the beam emittance in the experiment. The second equation is the definition of the betatron wavelength (λ_β):

$$\lambda_\beta = \frac{4\pi\gamma\beta mc}{e\,B_z}.$$ (2)

In the modulator, it is desired to maintain a constant radius beam, i.e. R" = 0. Given the beam energy, current, and emittance and having a fixed drift distance, $\lambda_\beta/4$, equations (1) and (2) can be used to determine the necessary magnetic field and expected beam radius. Unfortunately the aperture of the collimating slit at the end of the drift space establishes the maximum radius of the beam entering the output section. Measured values of the emittance indicated that the modulator would not be operated under its design specifications.

A number of simulations were performed using the relativistic klystron code RKS2[10] to determine the best values of drive power, solenoidal fields, and incident current to maximize rf current with no further modifications of the modulator. Results are shown in Figures 4 and 5 below. The measured emittance varied with the total dc current available at the entrance of the modulator. Fig. 4 shows the variation of generated rf current with solenoidal field for about 1.2 MW of deflection cavity drive and at four different values of emittance/current. Fig. 5 shows the variation of generated rf current with solenoidal field for an incident current of 1 kA with normalized emittance of 104 π-cm-mr and at four different deflection cavity drives. The maximum design deflection cavity drive was 1 MW, but earlier experiments on the Choppertron indicate that 1.2 MW drive levels could be maintained. For further simulations of the Choppertron we decided to use a 1-kA beam incident on the modulator with 1.2 MW of deflection cavity drive. A small increase in modulated current can be achieved in the simulations by ramping the axial magnetic field from 1.2 kG to about 2.2 kG over the last 20% of the modulator.
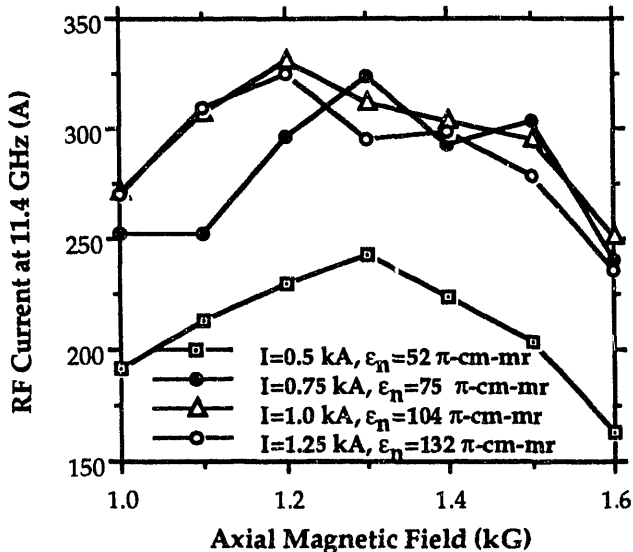

Figure 4. Predicted rf current for different beam emittances and dc currents, drive level = 1.2 MW.
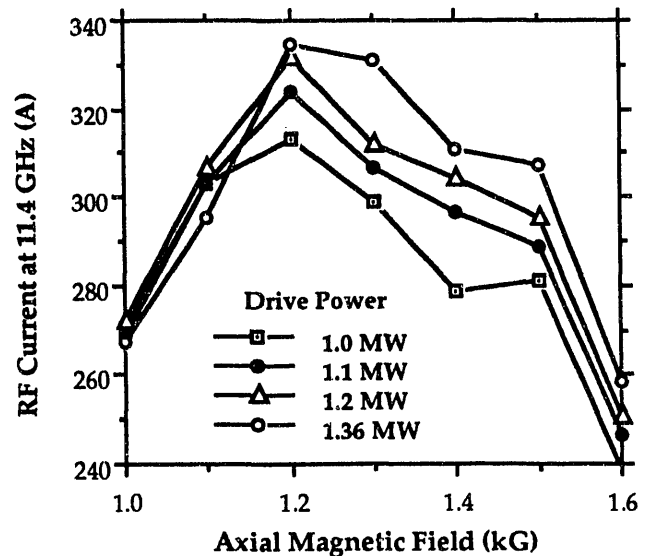
Figure 5. Predicted rf current for different drive levels of the deflection cavity, dc current = 1 kA.

2.3 Traveling-Wave Output Structures

The output section of the original Choppertron consisted of two identical 11.4-GHz traveling-wave output structures. One of these structures was replaced by a third structure with a de-Q-ing circuit to reduce the growth of transverse instabilities due to the excitation of higher order modes.[11] These transverse instabilities can lead to pulse shortening or beam breakup (BBU). For the reacceleration experiment all three of the above structures will be used. They will be referred to below as TW-1, TW-2, and TW-3 reflecting their placement in the experiment. TW-2, one of the original structures has been modified to add a de-Q-ing circuit. Figure 6 is a schematic of one of the original output structures. Figure 7 shows dispersion diagrams for TW-1 and TW-2

"extended" structures (calculated with URMEL for an infinitely repeating cell structure). The actual TW-1/TW-2 structures consist of only six/seven cells and have discrete resonances. TW-3 is a six cell structure with no de-Q-ing circuit and has a dispersion curve similar to TW-2. Table 1 list the design parameters of the three output structures.
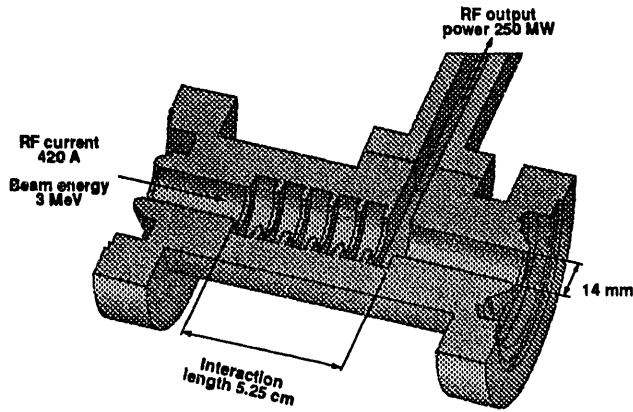

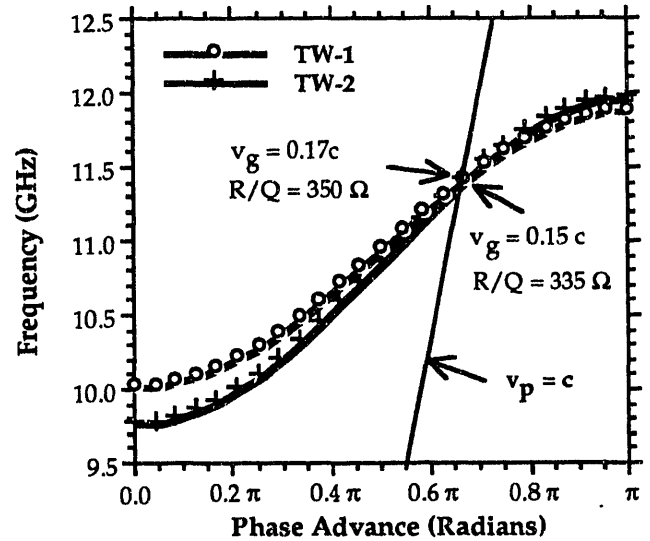Figure 6. Traveling-wave output structure,TW-3, with no de-Q-ing circuit.

Figure 7. Dispersion graph for monopole mode for the traveling-wave output structures.

Table 1. Parameters for traveling wave output structures.

Design Parameter	TW-1	TW-2 & TW-3
Resonant Frequency	11.424 GHz	11.424 GHz
Forward Traveling Mode	TM_{01}	TM_{01}
Number of Cavities (Total/Active)	6/4	7/5 & 6
Phase Shift per Cavity	120°	120°
Diameter of Beam Aperture	13.0 mm	14.0 mm
Fill Time for Fundamental Mode	1.35 ns	1.22 ns/1.05 ns
Harmonic Mean Group Velocity	0.13 c	0.167 c
RF Phase/Temperature Sensitivity	0.11 deg/°C	0.09 deg/°C
Demonstrated Output Power	120 MW	not tested/250 MW
Maximum Surface E-Field at 250 MW	120 MV/m	130 MV/m
BBU Frequency (HEM_{11} Lower Branch)	13.8 GHz	13.6 GHz
Estimated R/Q for BBU Mode	110 Ω	110 Ω

Simulations with RKS2 were performed to determine expected output levels and characteristics of the drive beam in the output section. Power levels determined by the simulations for the three extraction ports are shown in Fig. 8. The transient response time of the modulator drive cavity was not accounted for in the simulations. For the actual experiment, the rise time for the power output should be about 5 ns longer than shown, but the steady state values should not change. The output power is lower than expected for the modulated current (see Fig. 9). The traveling-wave structures were designed to produce 250 MW for 420 amperes of modulated current. We believe the lower power is due to uncertainty in modeling parameters. Results of tests[6] on the Choppertron with the first two traveling-wave structures and using a 5-MeV drive beam will be used to improve our modeling. Transport of the beam will be described in section 2.5.
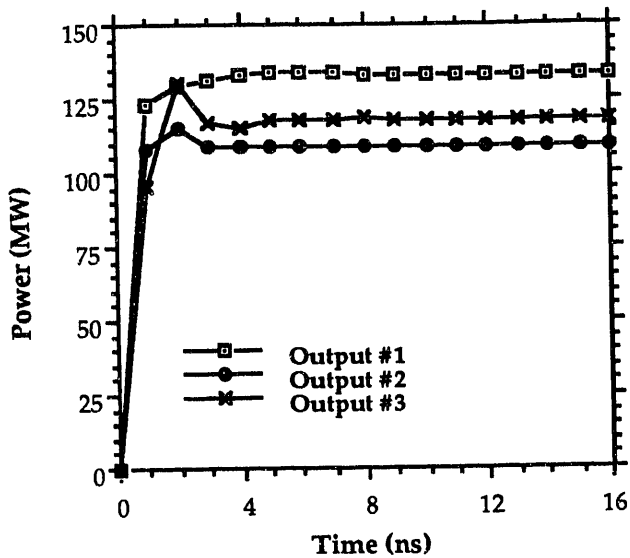
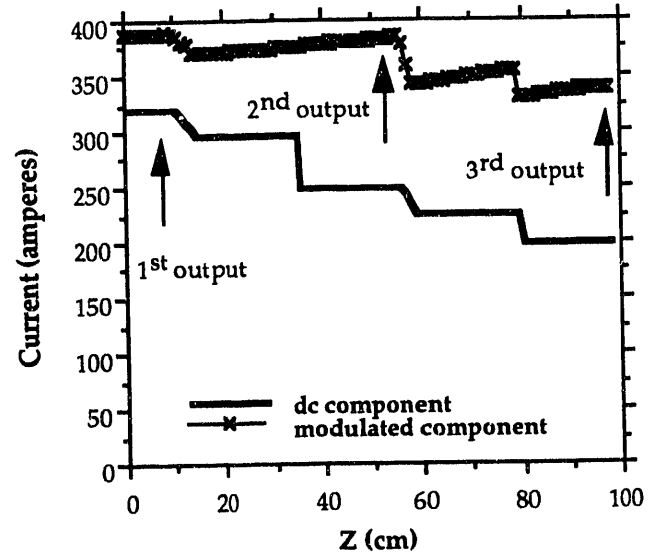Figure 8. Output power for each extraction structure.

Figure 9. DC and rf current in the output section.

2.4 INDUCTION CELLS FOR ACCELERATION OF MODULATED BEAM

The ATA induction cells produce an accelerating gap gradient of 250 kV and have an inner radius of 6.725 cm. To avoid large, abrupt variations in the beamline diameter, it was decided to place a sleeve in the reacceleration induction cells which would reduce the maximum radius to 1.5 cm, narrowing back to 7 mm prior to the accelerating gap (see the reacceleration induction cells in Fig. 1). In addition to maintaining a more uniform beamline radius, the sleeve permits the insertion of a current monitor and a steering coil within the induction cell. The reason for not maintaining a constant 7 mm radius was to ease beam transport as well as to allow sufficient aperture for installing a current monitor. The modified cells will have an accelerating gap gradient of 250 kV.

The resonant characteristics of the enlarged section of the sleeve was studied using URMEL. There was initial concern that these sections could act as rf cavities and disrupt the beam. The results of URMEL showed that the enlarged sections would have negligible effect on the beam. In simulations where the beam tube radius changed immediately in value, resonances with modest R/Q's and Q's were found. The largest R/Q's (Q's) were about 11 Ω (3,200 to 2,200) at 8.7 GHz and 16.4 GHz for monopole modes and 2.5 Ω (3,000) at 12.2 GHz for dipole modes. A tapered radius produced significantly smaller R/Q's. No resonances were found near the modulation frequency (11.4 GHz), the BBU resonance (800 MHz) of the ATA cell,[12] or the BBU resonance (13.6 GHz) of the traveling-wave structures. Simulations using scattering matrix formulation[13] indicated that the abrupt transition, compared to a tapered, would significantly reduce rf power transmission through the beam line over the frequency spectrum of interest. Reduced rf transmission can be advantageous as electromagnetic coupling of the various beamline structures can lead to regenerative beam instabilities. For our proposed design we have assumed that these sections will prevent electromagnetic coupling between the traveling-wave structures.

A time-domain, electromagnetic simulation computer code, AMOS,[14,15] was used to study the effects of the accelerating gap on the transiting beam. Over many induction cells, monopole resonances in the gaps could cause longitudinal instabilities of the beam and extractable power loss. The dipole resonances are a greater concern as they contribute to the transverse instability of the beam. However, computer simulations similar to those mentioned in Section 2.5 indicated that these effects would be negligible in the proposed experiment. Both monopole and dipole impedances were calculated and the results are shown in Figures 10 and 11. The small beam pipe traps numerous resonant modes within the gap. Calculated power loss due to interaction of the modulated beam with the monopole resonances is about 2.4 MW or about 2.8% of the power increase from the induction cell. As shown in Fig. 11, there are three relatively strong dipole resonances near 10 GHz. Simulations were performed to verify that these resonance would have negligible interaction with the 11.4 GHz modulated current beam.
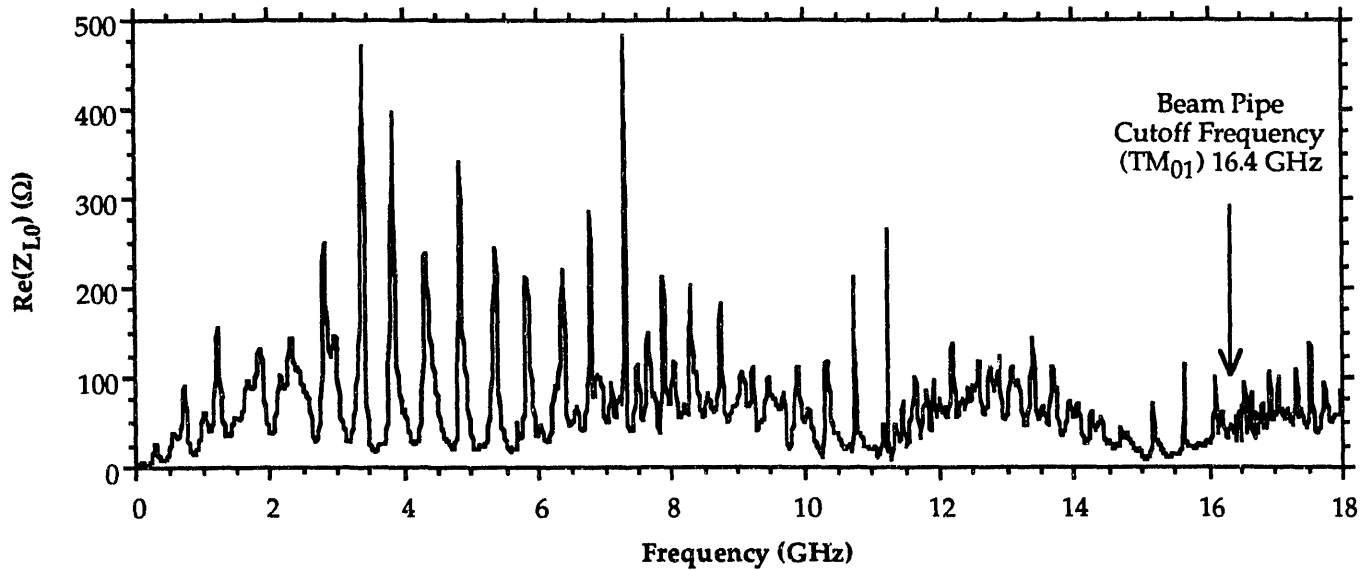
6

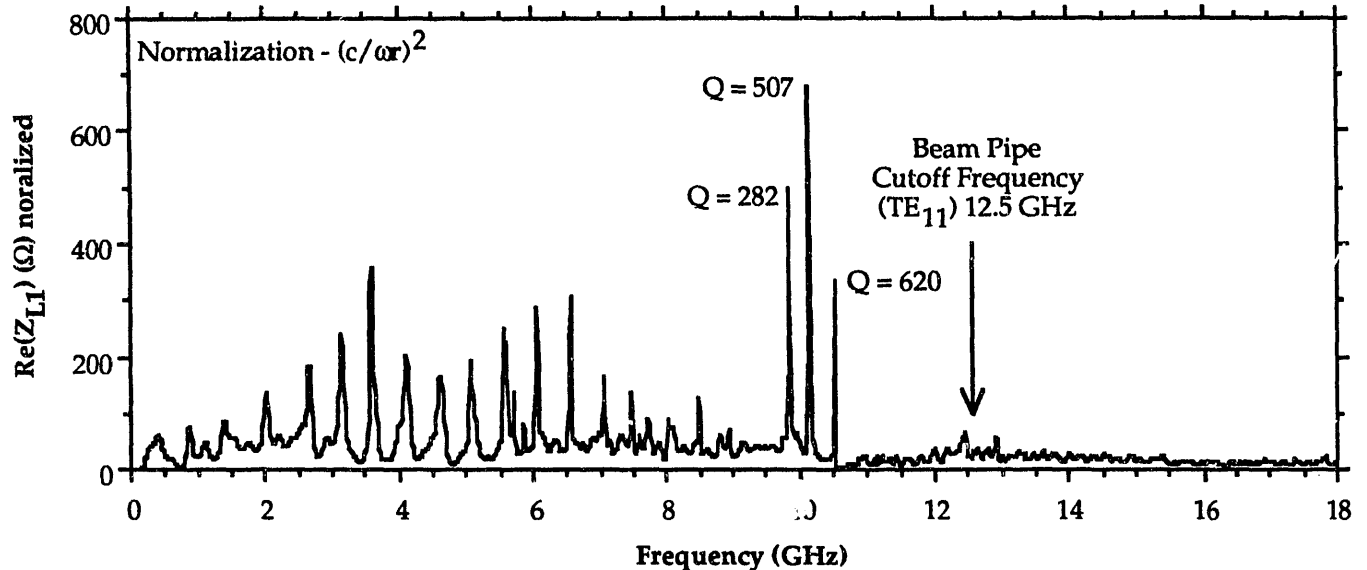Figure 10. Monopole impedance $Re(Z_{L0})$ versus frequency for the modified ATA cell.

Figure 11. Dipole impedance $Re(Z_{L1})$ versus frequency for the modified ATA cell.

2.5 BEAM TRANSPORT THROUGH OUTPUT SECTION

Transporting the drive beam through the output section was a critical issue due to the large expected energy spread over the "rf bucket." During the 2.5 MeV Choppertron experiments about 90% of the current could be transported with the drive modulator off. However, the solenoidal fields that produced the highest output powers only transported about 70% of the incident current when the drive modulator was off. Above certain current levels excitation of higher order modes had led to pulse shortening or beam breakup. As the geometry of the reacceleration experiment was more complex than the Choppertron, we felt it was necessary to use the RKS2 klystron code to accurately model the transport of the beam. The BBU Code[16] was used to determine the growth of transverse instabilities.

The RKS2 simulations attempted to model the placement and maximum current levels of the solenoids as accurately as possible. However, the code does not take into account permeable materials such as the magnetic shields and ferrite expected in the actual experiment. Results of the transport simulations are shown in Fig. 12.

7

The average axial magnetic field associated with Fig.12 was about 2.2 kG. The abrupt change in radius at 35 cm and 77 cm into the output section is due to beam loss as the beam line radius narrows prior to the acceleration gap. The transport was optimized for the lower energy, synchronous electrons which comprise the "rf bucket." The majority of the current loss is due to higher energy electrons in the microbunch. This effect explains the large loss of dc current as compared to the relatively constant modulated current shown in Fig. 9. The small increase in modulated current with distance seen in Fig. 9 is caused by the energy spread across the microbunch imposed by the traveling-wave structure. An important effect on current transport simulated by the RKS2 code is the radial defocusing of electrons that lag in phase with respect to the microbunch during transit of the traveling-wave structures. Fig. 13 illustrates the growth of the radius envelope for the beam in a traveling-wave structure as compared to a drift tube.
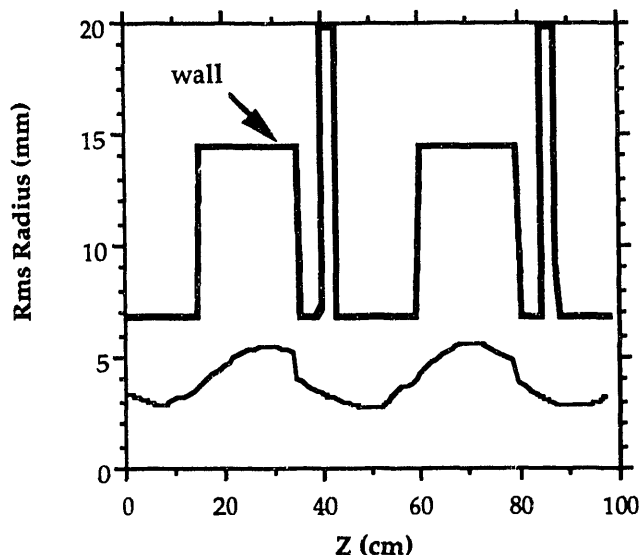

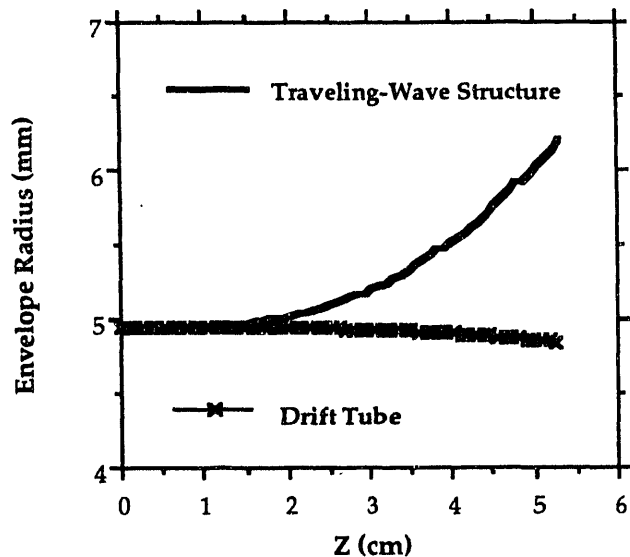Figure 12. Beam radius (rms) in the output section.

Figure 13. Effect of the traveling-wave electromagnetic fields on beam radius.

Dispersion diagrams for the dipole mode of TW-1 and TW-2 are shown in Fig. 14. Excitation of higher order modes, specifically the lower HEM_{11} branch near the phase velocity equalling the speed of light, resulted in regenerative beam breakup in the original Choppertron experiments. The use of de-Q-ing circuits to
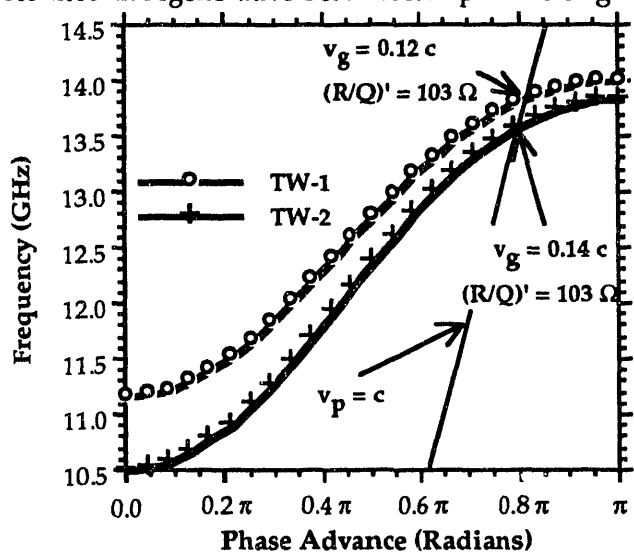

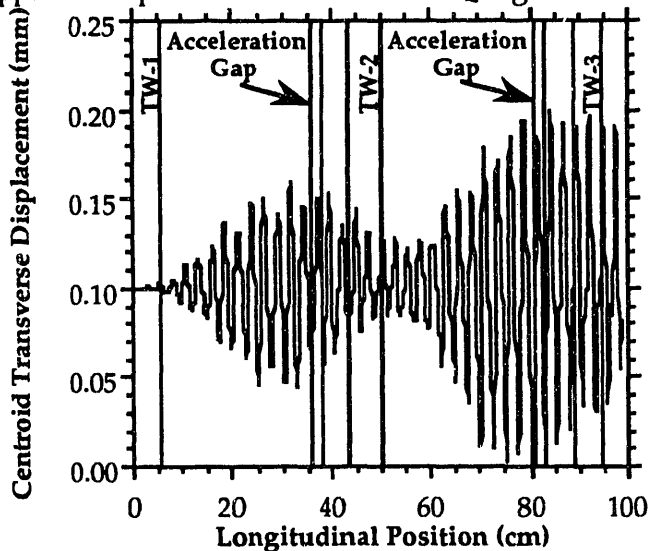Figure 14 Dispersion graph for dipole mode (lower HEM_{11} branch) for the traveling-wave structures.

Figure 15. Transverse displacement of the beam centroid in the output section of the experiment.

8

aggressively damp these modes was successful,[17] and the first two output structures of the reaccelerationexperiment will have de-Q-ing circuits. Fig. 15 shows a simulation of the transverse displacement of the beam's centroid as a function of position along the axis of the output section at 30 ns into the beam pulse. No further growth in the transverse displacement was noted for the remainder of the 50 ns current pulse. For the simulation the beam was assumed to enter the output section parallel to the axis and with a constant displacement of 0.1 mm. The rf current was increased linearly from zero to 420 amperes in 5 ns, remained at 420 amperes for 40 ns, and then decreased to zero over 5 ns. A constant axial 2 kG magnetic field was used for focusing. The positions of the three output structures and two accelerating gaps are shown in Fig. 15 for reference. TW-1 imparts a transverse momentum which causes the beam to begin a betatron oscillation and also introduces an energy spread over the microbunches. Although not obvious in this simulation, phase mixing due to energy spread and betatron oscillation is expected to be an important effect in damping transverse instabilities in a RK-TBA.[17] For our design, we expect modest growth of the transverse displacement which will not cause beam disruption.

3. SUMMARY/IMPLICATIONS OF MODELING

A comprehensive design of an experiment to study the reacceleration of a modulated beam using computer simulations has been performed. Our simulations indicate that approximately 250 MW/m can be achieved. The area of greatest difficulty for the experiment is expected to be due to the initial beam emittance. The emittance, which is larger than design specifications for the Choppertron modulator, limits the maximum modulated current, possibly will lead to greater than expected emittance growth in the modulator, and increases the difficulty of transporting the beam through the output section. All these effects reduce the extractable power from the beam. The two reacceleration induction cells should not adversely effect the electron beam dynamics. However, a completely redesigned induction cell which takes advantage of the small bore of the beam line and has significantly reduced impedance characteristics is needed for larger reacceleration experiments. Similarly, the growth of transverse instabilities caused by the traveling-wave structures should not be significant for this experiment, but will require further study as the number of output structures is increased. We intend to use data from a currently operating experiment on the Choppertron[6] as it becomes available to improve our modeling and recommend design improvements.

4. ACKNOWLEDGMENTS

We would like to thank J. Haimson and B. Mecklenburg for their valuable advice on the Choppertron modulator and traveling-wave output structures. Special thanks is given to A. Sessler, G. Westenskow, and S. Yu for their assistance in determining experimental goals and maintaining realism in our design. We thank C. Shang and G. Craig for their help in modeling the modified ATA induction cells. For engineering and technical assistance, we thank S. Hawkins and C. Holmes.

5. REFERENCES

1   J. Haimson and B. Mecklenburg, "Design and Construction of a Chopper Driven 11.4 GHz Traveling Wave RF Generator," Proceedings of the 1989 IEEE Particle Accel. Conf., pp. 243-245.

2   T.L. Houck, et al., "Relativistic Klystron Research for Two-Beam Accelerators," SPIE Symposium on Intense Microwave and Particle Beams II Proceedings Vol. 1629-47 (1992).

3   T.L. Houck and G.A. Westenskow, "Status of the Choppertron Experiments," Proceedings of the 16th Int'l LINAC Conference, Ottawa, Ontario, Canada, Aug. 23-28, 1992.

4   A.M. Sessler and S.S. Yu, "Relativistic Klystron Version of the Two-Beam Accelerator," Phys. Rev. Lett., 58, 2439, 1987.

5   S. Humphries, Jr., Principles of Charged Particle Acceleration, pp. 288-301, Wiley, New York, 1985.

6   T.L. Houck and G.A. Westenskow, "Status of an Induction Accelerator Driven, High-Power Microwave Generator at Livermore,"SPIE Proceedings Vol. 1872-16, 1993.

[7] E.P. Lee and R.K. Cooper, "General Envelope Equation for Cylindrically Symmetric Charged-Particle Beams," Particle Accelerators, 7, 83 (1976).

[8] E.P. Lee, S.S. Yu, and W.A. Barletta, "Phase-Space Distortion of a Heavy-Ion Beam Propagating Through a Vacuum Reactor Vessel," Nuclear Fusion, 21, No. 8, 1981.

[9] J. Haimson and B. Mecklenburg, Chopper Driven Traveling Wave Relativistic Klystron Design Report, Report No. HRC-774, Haimson Research Corporation, Palo Alto, CA, 1988.

[10] R.D. Ryne and S.S. Yu, "Relativistic Klystron Simulations Using RKTW2D," Proceedings of the 15th Int'l LINAC Conference, Albuquerque, NM, Sep. 10-14, 1992, pp. 177-179. RKTW2D has been furthered developed and an updated manual, G.M. Fiorentini, User's Guide for the Relativistic Klystron Simulation Programs RKS1 and RKS2, is available through the LBL Collider Physics Group.

[11] J. Haimson and B. Mecklenburg, "Suppression of beam induced pulse shortening modes in high power RF generator and TW output structures," SPIE Symposium on Intense Microwave and Particle Beams II Proceedings Vol. 1629-71 (1992).

[12] G.J. Caporaso, "The Control of Beam Dynamics in High Energy Induction Linacs," Proceedings of the 13th Int'l LINAC Conference, Stanford, CA, Jun. 2-6, 1986, pp. 17-21.

[13] J.M Neilson, P.E. Latham, M. Caplan, and W.G. Lawson, "Determination of the Resonant Frequencies in a Complex Cavity Using the Scattering Matrix Formulation," IEEE Trans. Microwave Theory Tech., 37 No. 8, 1989, pp. 1165-1170.

[14] J.F. Deford, G.D. Craig, and R.R. McLeod, "The AMOS wakefield code," Proceedings of the Conference on Computer Codes and the Linear Accelerator Community, Los Alamos, NM, 1990, pp. 265-289.

[15] G.D. Craig, "Wake Potentials and Impedances for the ATA Induction Cell," Proceedings of the 15th Int'l LINAC Conference, Albuquerque, NM, Sep. 10-14, 1990, pp. 381-383.

[16] T.L. Houck, G.A. Westenskow, and S.S. Yu, "BBU Code Development for High-Power Microwave Generators," Proceedings of the 16th Int'l LINAC Conference, Ottawa, Ontario, Canada, Aug. 23-28, 1992.

[17] G.A. Westenskow, T.L. Houck, and S.S. Yu, "Transverse Instabilities in a Relativistic Klystron Two-Beam Accelerator," Proceedings of the 16th Int'l LINAC Conference, Ottawa, Ontario, Canada, Aug. 23-28, 1992.